Carbohydrate Polymers 79 (2010) 614–619

Contents lists available at ScienceDirect

Carbohydrate Polymers

journal homepage: www.elsevier.com/locate/carbpol

Preparation of all-cellulose composite by selective dissolving of cellulose surface in PEG/NaOH aqueous solution

Donglin Han, Lifeng Yan *

Hefei National Laboratory for Physical Sciences at the Microscale, Department of Chemical Physics, University of Science and Technology of China, Hefei 230026, PR China

ARTICLE INFO

Article history:
Received 24 July 2009
Received in revised form 30 August 2009
Accepted 11 September 2009
Available online 18 September 2009

Keywords:
All-cellulose
Film
Transparent
Strength

ABSTRACT

Here, PEG/NaOH aqueous solution, a recently reported solvent system for cellulose was utilized to prepare an all-cellulose composite. The composite was produced from commercial filter paper by converting a selective dissolved fiber surface into a matrix. The morphology, crystalline structure, mechanical and optical properties of this composite was investigated by the wide-angle X-ray diffraction (WAXD), scanning electron microscopy (SEM), universal tensile tester, and optical microscope. The results revealed that the all-cellulose composites had a high mechanical performance and an optical transparency. The effect of processing conditions on the interfacial bonding and therefore the mechanical performance of the final composites has also been investigated.

1. Introduction

Polymer composite materials have been attracted much attention for their mechanical properties and light-weight, and they were widely used in various applications, including commodities (Tsai & Hahn, 1980), aerospace vehicles (Chermant, Fantozzi, & Naslain, 2000), smart devices (Miravete, 1997) and so on. New applications also call for many new requirements concerning their mechanical properties, transparency, environmental sensitivity and biocompatibility (Bledzki & Gassan, 1999).

Cellulose, the most affluent biopolymer resource in the world, is widely considered as a nearly inexhaustible raw material with fascinating structures and properties for the remarkable demand of environmentally friendly and biocompatible products (Klemm, Heublein, Fink, & Bohn, 2005; Klemm et al., 2006; Nishio, 2006). As it is well known, cellulose is the main reinforcing constituent in plant cell walls, and it is a natural linear polysaccharide in which D-glucopyranose rings are connected to one another with β-(1,4)-D-glycosidic links. In recent years, fully recyclable all-polypropylene composites (all-PP) have been proposed to replace traditional glass fiber reinforced plastics for a number of applications, notably the automotive industry (Alcock, Cabrera, Barkoula, Loos, & Peijs, 2006; Cabrera, Alcock, Loos, & Peijs, 2004). Following the success of all-polymer composites like all-PP, the concept of all-cellulose composite of which both the matrix and fibers originate from cellulose-based feedstocks has received increasing attention (Gindl & Keckes, 2005; Gindl, Martinschitz, Boesecke, & Keckes, 2006; Lu, Zhang, Rong, Yue, & Yang, 2004; Nishino & Arimoto, 2007; Soykeabkaew, Nishino, & Peijs, 2009; Zhao et al., 2009). Due to the inherent compatibility between the matrix and fibers, excellent interfacial bonding and thus more powerful reinforcing effect can be anticipated in this type of composites. Although tremendous effort has been paid to obtain the realization of this concept, limitations still exist because matrix cellulose in its native state cannot be processed by solution or melt processing technique due to the strong hydrogen bonding (inter- and intra-molecular). Some research groups have followed the approach similar to the fashion of all-PP composites where cellulose fibers are impregnated with a cellulose matrix to manufacture all-cellulose composite (Lu, Zhang, Rong, Shi, & Yang, 2002; Nishino, Matsuda, & Hirao, 2004).

Up to now, several kinds of solvent systems have been accepted to be capable of dissolving cellulose, such as calcium and sodium thiocyanate (Hattori, Koga, Shimaya, & Saito, 1998), lithium chloride/*N*,*N*-dimethylacetamide (LiCl/DMAc) (McCormick, Callais, & Hutchinson, 1985), dimethyl sulfoxide (DMSO)/tetrabutylammonium fluoride (Heinze et al., 2000), NH_3/NH_4SCN (Cuculo, Smith, Sangwatanaroj, Stejskal, & Sankar, 1994), NaOH/urea (Zhang, Ruan, & Zhou, 2001), ionic liquids (Swatloski, Spear, Holbrey, & Rogers, 2002), PEG/NaOH (Yan & Gao, 2008), etc. These developments concerning the novel solvents for cellulose offer the possibility to prepare all-cellulose composite through a solution processing which is based on surface selective dissolution of natural cellulose fibers (Soykeabkaew, Arimoto, Nishino, & Peijs, 2008). During the composite preparation, the surface layer of the cellulose fibers is partially dissolved to form the matrix phase of the composites. Meanwhile, the cores maintain their original structure and impart a reinforcing effect to the composite. This method is not only

* Corresponding author. Tel.: +86 551 3606853; fax: +86 551 3602969.
E-mail address: lfyan@ustc.edu.cn (L. Yan).

0144-8617/$ - see front matter © 2009 Elsevier Ltd. All rights reserved.
doi:10.1016/j.carbpol.2009.09.008

simplifies the composite's preparation process but also provides a significantly improved fiber/matrix interface (Nishino & Arimoto, 2007; Nishino et al., 2004; Soykeabkaew et al., 2009). It is testified that all-cellulose composites showed excellent mechanical properties similar or better as those prepared by a traditional impregnation method (Nishino et al., 2004; Qin, Soykeabkaew, Xiuyuan, & Peijs, 2008; Soykeabkaew et al., 2009).

Recently Nishino et al. prepared the all-cellulose composite from pure cellulose and ramie fibers in LiCl/DMAc system (Nishino et al., 2004; Soykeabkaew et al., 2009). Gindl et al. prepared an optically transparent all-cellulose composite from microcrystalline cellulose (MCC) with the same solvent system (Gindl & Keckes, 2005; Gindl et al., 2006). Zhao et al. manufactured the all-cellulose composite in ionic liquids (Zhao et al., 2009). Obviously, it is a challenge to manufacture all-cellulose composites with a novel solvent which is environmental friendly and energy efficient.

In this study, we prepared all-cellulose composite from conventional filter paper by using PEG/NaOH aqueous solution which has been a new "green" solvent system for dissolving cellulose (Yan & Gao, 2008). The surface selective dissolution method for the manufacturing of all-cellulose composites was applied (Nishino & Arimoto, 2007). In addition, since both fiber and matrix are composed of the same material they show excellent interfacial compatibility. The effect of the immersion time of the fibers in the solvent during composite preparation on the properties of the all-cellulose composites was systematically investigated. The structure and morphology of the prepared composites were examined by using scanning electron microscopy and X-ray diffraction. Tensile testing was used to characterize the mechanical and thermal properties of the composites. The optical property was also studied.

2. Experimental

2.1. Materials

Filter paper (100% α cellulose) with density of 115 g/m^2 and thickness of 0.20 ± 0.01 mm was supplied by Hoyang Co. Ltd. (Hangzhou, China).

All the reagents (PEG-2000 and NaOH) of analytical grade were purchased from Sinopharm Chemical Reagent Co. Ltd. in China and were used as received without further purification. Ultrapure water with resistivity of 18 MΩ cm was produced by a Milli-Q (Millipore, USA) and was used for solution preparation.

2.2. Sample preparation

The preparing process of the all-cellulose was selective dissolving of the surface of the cellulose fibers. At first, the filter paper was immersed in ultrapure water for 24 h at 25 °C and dried in vacuum at 35 °C for more than 12 h. Judging from an X-ray diffraction pattern of the filter paper, no structural change was observed after the pretreatment. Then 1.0 g of PEG-2000 and 9.0 g of NaOH were added into 90 ml of ultrapure water to prepare the aqueous solution of PEG/NaOH. Next, the pretreated filter paper was immersed in the aqueous solution at room temperature for 1 h, and then the mixture was cooled to −15 °C and held at that temperature for 2–12 h. The effect of the immersion time at low temperature on the structure and properties of the final all-cellulose composite was systematically investigated. Then, the treated filter paper, with a selectively dissolved fiber surface, was compressed between two poly(tetrafluoroethylene) plates at 0.1 MPa for 1 h (Nishino & Arimoto, 2007), followed by immersion in ultrapure water several times to make sure the NaOH and PEG were completely removed from the obtained composites. During the processes, the fibers were unified and re-solidified, and an all-cellulose composite was obtained. Finally, the all-cellulose composite was dried in a vacuum at 50 °C for 24 h for further experiment. Therefore, a series of all-cellulose composites were prepared (Table 1).

2.3. Characterization

T_g of the samples were measured using a differential scanning calorimetry (DSC, Perkin-Elmer DSC-4, Norwalk, CT). The measurement was performed with a heating rate of 20 °C/min from 20 to 200 °C. DTG curves were obtained by Shimadzu TGA-50 thermogravimetric instrument. The temperature range employed is 30–700 °C with a heating rate of 10 °C/min.

To clarify the crystal structure of the composites, time-resolved synchrotron WAXD measurements were performed on a setup with Mar 345 image plate as detector and the Cu Kα was used as the source (wavelength $\lambda = 0.1542$ nm). The experiments were performed at national synchrotron radiation laboratory (NSRL) in China. The Fit2D (http://www.esrf.fr/computing/scientific/FIT2D/) software package was used to analyze the two-dimensional WAXD patterns. The mass fraction F_X of a specific crystal form X is calculated on the basis of peak fitting during which a 2θ range from 6° to 36° was taken, and the scanning speed is 2.0°/min. The mass fraction F_X is defined as the ratio between the diffraction intensity of X crystals $\sum A_X$ and the total intensity $\sum A_T$ in the 2θ range, as expressed in the following equation:

$$F_X = \frac{\sum A_X}{\sum A_T}$$

The surface structures of the composites were measured using a Shimadzu SEM (Superscan SSX-550, Japan). The apparatus is equipped with a low vacuum system which allows to directly measuring the samples without gold coating.

The tensile strength (σ_B) and elongation at break (ε_B) of the composites were measured on a universal tensile tester (TS7104, Shenzhen SANS Test machine, China) according to ISO527-3:1995 at a speed of 5.0 mm/min. The specimens were in rectangular shape with dimension of 20 × 5 × 0.2 mm. The length between two grips was set as 10 mm. Each testing was repeated on five specimens and the mean values as well as standard deviation were reported.

Contact angles of the samples were measured by a contact angle goniometry (JC2000C, Zhongcen, Shanghai, China) at room temperature.

VIS-721 spectrophotometer (Shanghai, China) was used to determine the transparency of the composites at a wavelength of 540 nm.

3. Results and discussion

Firstly, we should investigate whether the prepared sample is pure cellulose or a blend of cellulose with PEG. DSC measurements were carried out to determine the glass temperature of the composite. As shown in Fig. 1, for pure PEG there appears a strong peak at about 58 °C, which corresponds to the phase transition of PEG during melting. However, for the as-prepared composite, there is

Table 1
A series of composites with immersion times increasing gradually.

Sample code	Immersion time in the thawed solution (h)	Mechanical pressure (MPa)
Filter paper	0	0
Composite-1	1	0.1
Composite-2	3	0.1
Composite-3	6	0.1
Composite-4	12	0.1

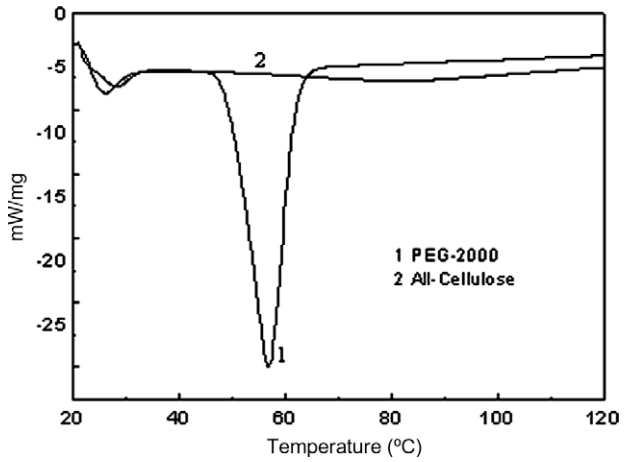

Fig. 1. DSC curves of PEG-2000 and the as-prepared all-cellulose composite.

no peak at all near the position, indicates the PEG molecule in the solvent was washed out completely and the as-prepared material is a composite full of cellulose. TGA curves of the as-prepared samples, cellulose and the pure PEG and DGA curves of as-prepared samples and pure PEG are also the evidence to confirm the complete removal of PEG, as shown in Fig. 2. The peak at about 322 °C in the curves of the as-prepared all-cellulose sample is corresponding to the decomposition of the pure cellulose. As a contrast, the peaks at about 395 °C in the curves of PEG-2000 is belonged to the decomposition of PEG-2000. Obviously, there is no peak at all at about 395 °C in the curve of the as-prepared all-cellulose sample.

3.1. Crystalline structure

Fig. 3 shows the X-ray diffraction photograph of the filter paper and the all-cellulose film (Composite-4). Typical 2D detector images for the filer paper (A) clearly showed the Debye–Scherrer rings assigned as cellulose I modification. However, the diffraction pattern of the all-cellulose composite (B) became diffuse, indicates a decrease in the crystalline degree by the selective dissolving and re-solidification process. Fig. 4 shows the one-dimensional WAXD intensity curves of these two composites. Clearly, the pattern of filter paper exhibits the typical diffraction peaks at 14.8°, 16.2°, 22.7°, and 34.3°, which belong to the crystalline structure of cellulose I (Nishiyama, Langan, & Chanzy, 2002). In contrast, the WAXD pattern of the all-cellulose composite (Composite-4) only demonstrates two overlapping diffractions at $2\theta = 19.7°$ and 21.9°, suggests that the regeneration part (cellulose II) appeared and laid over the native cellulosic fibers (cellulose I). In addition, a widening of diffraction line appeared at around 20°, indicates that the regeneration part (cellulose II) turned into noncrystalline regions in the composite with the dissolving of the cellulose fibers gradually. However, the main peaks at $2\theta = 34.3°$ remained in the all-cellulose

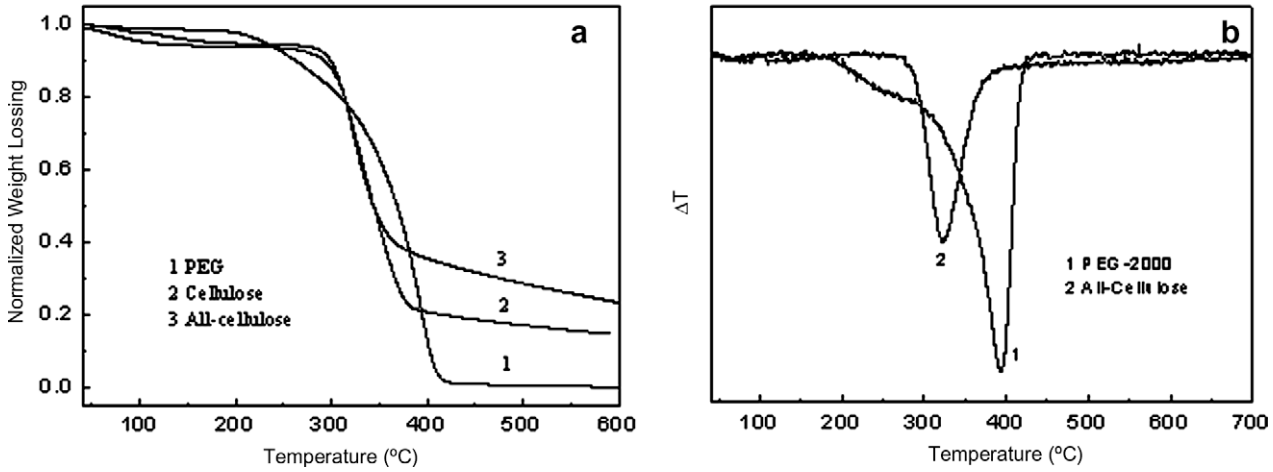

Fig. 2. (a) TGA curves of cellulose, PEG-2000 and the as-prepared all-cellulose composite. (b) DGA curves of PEG-2000 and the as-prepared all-cellulose composite.

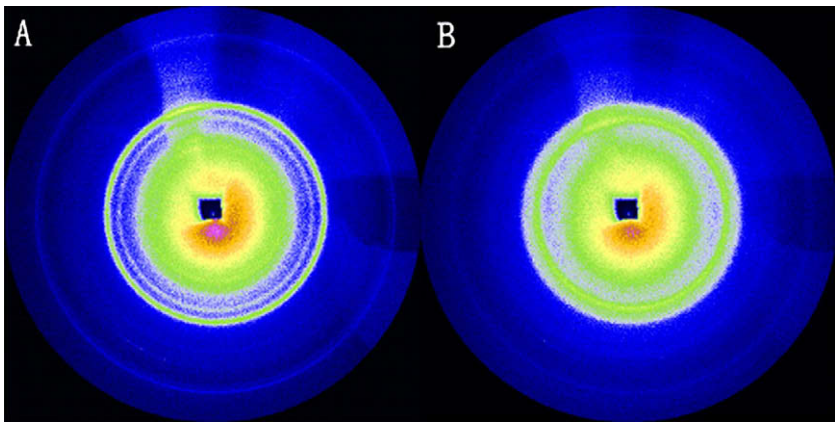

Fig. 3. Representative WAXD 2D detector images acquired at the filter paper (A) and the all-cellulose composite (B).

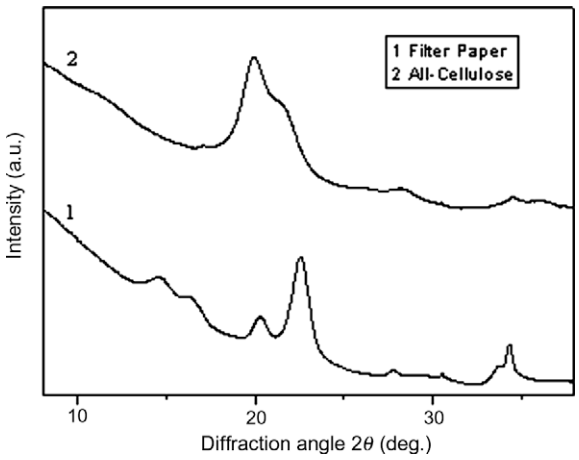

Fig. 4. Wide-angle X-ray diffraction profiles of the filter paper and the all-cellulose composites.

composite profiles which demonstrated that the crystal modification of cellulose I was sustained in the composite, reflecting the existence of the residual fibers. In addition, the constant peak positions of the crystalline reflections indicate that the molecular distances remain unchanged in the crystalline regions. The results of the curve fitting were recognized on the figure for the filter paper and the all-cellulose composites, where the crystalline 1 0 1, 1 0 −1, 0 0 2 and 0 4 0 reflections were shown with the numeral character (Egusa, Kitaoka, Goto, & Wariishi, 2007; Hult, Iversen, & Sugiyama, 2003; Moharram & Mahmoud, 2007).

3.2. Mechanical properties

The typical stress–strain (σ *vs* ε) curves for filter paper and Composite-1–4 were presented in Fig. 5 and the correlative data were summarized in Table 2. Compared with the filter paper, the tensile strength at break of the all-composites increased gradually with the immersion time, whereas their elongation at break (ε_B) changes slightly. This suggested that the treatments can effectively improve the mechanical strength of the composites. Moreover, with an increase in the immersion time from 1 to 3 h, the σ_{max} values sharply increased from (38.0 ± 2.9) MPa to (59.3 ± 6.0) MPa. This strong dependence of the tensile strength on the immersion time was probably related to the surface fibers intensively dissolving and re-solidifying, indicates an effective adhesion between the fibers. On the other hand, for the Composite-3 and Composite-4, the fiber surfaces were efficiently dissolved, the σ_{max} value increased a little with immersing for more than six hours.

The Young's modulus of the composites were plotted as a function of the immersion time, as showed in Fig. 6. For all the composites, the Young's modulus increased gradually with the immersion time, indicating that the more fibers are transformed into matrix, the more brittle they are (Nishino & Arimoto, 2007).

Appropriate understanding of structure–mechanical property relationships in the all-cellulose composite is based on the proper structural information. SEM measurements provide direct information regarding the interfacial bonding of these composites, as shown in Fig. 7. In Fig. 7(A), a surface micrograph of filter paper was presented, and a fine weblike, and highly fibrous network structure was apparent. Each fiber was observed, and the typical lateral dimension is 10–20 μm. The surface structure of Composite-1 was showed in Fig. 7(B), and the fiber was partially disentangled and then dissolved, so the fibrous network structure was successfully fractured in the cooling solution and the all-cellulose composites were generated originally. It could be found that the fiber/matrix interface turned to be obscure (Nishino et al., 2004). For the Composite-2, most of the fiber/matrix interface was diminished (Fig. 7(C)), and there was little pore remained in the surface of the composite. Associated with the stress–strain curve of this composite, the tensile strength was expected to be enhanced due to greater fiber/matrix adhesion. Besides, with the decrease of the amount of the pores, the extension of the composites gets

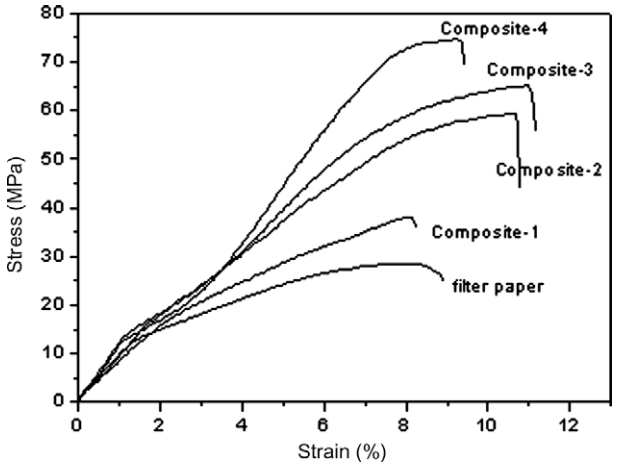

Fig. 5. Stress–strain curve of the prepared composites.

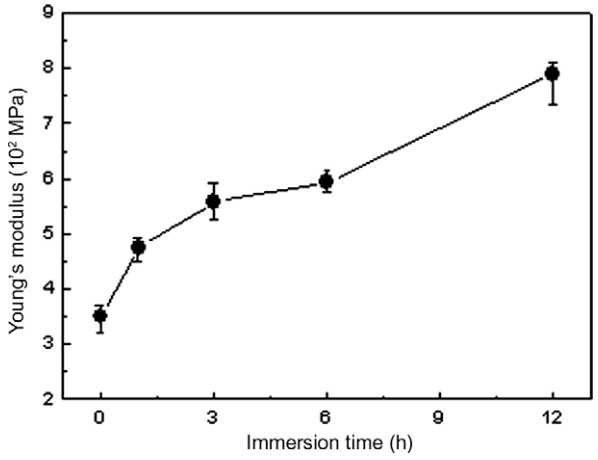

Fig. 6. Relationship between the Young's modulus and the immersion time for the all-cellulose composites.

Table 2
Mechanical properties of the prepared composites.

Sample code	Stress at max (σ_{max}) (MPa)	Strain at max (ε) (%)	Strain at break (ε_B) (%)
Filter paper	28.5 ± 3.4	8.1 9 ± 0.98	8.94 ± 1.02
Composite-1	38.0 ± 2.9	8.1 0 ± 1.26	8.26 ± 1.35
Composite-2	59.3 ± 6.0	10.65 ± 1.47	10.77 ± 1.19
Composite-3	65.3 ± 4.8	11.01 ± 1.09	11.17 ± 0.88
Composite 4	74.7 ± 5.6	9.26 ± 1.33	9.42 ± 1.11

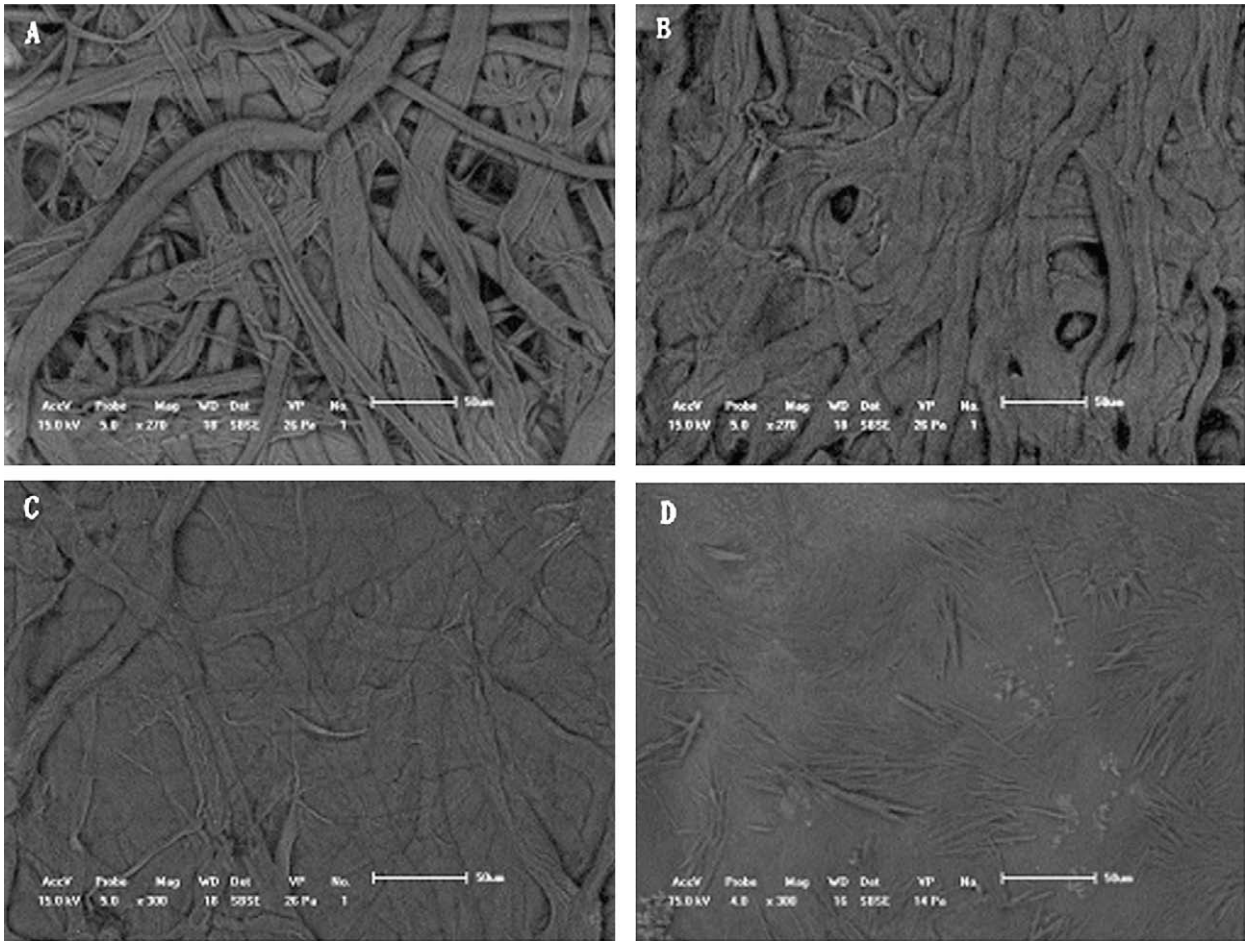

Fig. 7. SEM micrographs of (A) filter paper, (B) Composite-1, (C) Composite-2 and (D) Composite-4 (all the scale bar is 50 μm).

weaker. Therefore, they became more brittle. From the SEM of the Composite-4 as shown in Fig. 7(D), it could be found that the treated surface exhibits high level of homogeneity and the inter-diffusion of the cellulose molecules across the interface were ready to be stimulated. This indicated that the fibers were completely unified in the composite by selective dissolving of the fiber surface and compression followed by re-solidification, and the all-cellulose composite was produced.

It is well known that the filter paper is high hydrophilic. However, the hydrophobicity of the all-cellulose composites was increased. The contact angle of the all-cellulose Composite-4 is 55°, as shown in Fig. 8. It suggested that the structure of the all-cellulose was more compact than that of the filter paper.

3.3. Transparency

Note that the all-cellulose composites have not only improved mechanical strength but also good optical transparency. Fig. 9 shows the optical photographs of the filter paper and the all-cellulose composites. The thickness of these composites is (0.2 ± 0.01) mm. At the wavelength of 540 nm, the transmittance of Composit-0, Composite-2 and Composite-4 were 0.6%, 8.5% and 12.9% respectively.

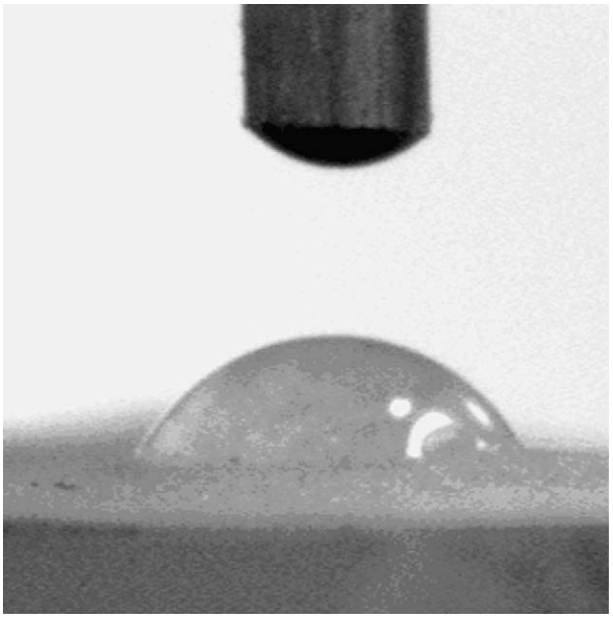

Fig. 8. Contact angle measurement with water and the surface of the composites.

4. Conclusions

A kind of novel all-cellulose composite based on conventional filter paper has been successfully prepared by using PEG/NaOH aqueous solution as solvent. When the filter paper was immersed in the pre-cooling solution more than six hours, the all-cellulose composites are molding. Such composite has possessed a nice interface between the remaining fibers and the surrounding matrix

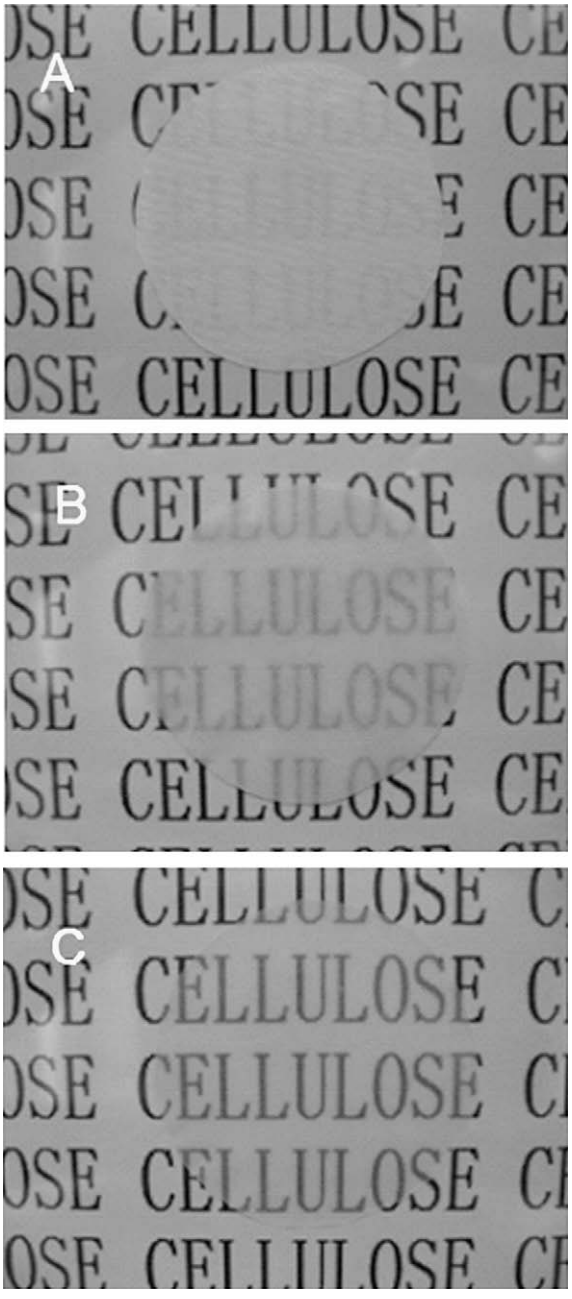

Fig. 9. Optical photographs of filter paper (A), Composite-2 (B) and Composite-4 (C).

from the selectively dissolved and re-solidified fiber surface, which results in an excellent bonding, a high mechanical performance and an optical transparency. In addition, the all-cellulose composite is totally composed of sustainable cellulosic resources, so it is biodegradable after service.

Acknowledgements

This work is supported by the National Natural Science Foundation of China (No. 20874095) and the National Basic Research Program of China (No. 2007CB210201).

References

Alcock, B., Cabrera, N. O., Barkoula, N. M., Loos, J., & Peijs, T. (2006). The mechanical properties of unidirectional all-polypropylene composites. *Composites Part A Applied Science and Manufacturing, 37*(5), 716–726.

Bledzki, A. K., & Gassan, J. (1999). Composites reinforced with cellulose based fibres. *Progress in Polymer Science, 24*(2), 221–274.

Cabrera, N., Alcock, B., Loos, J., & Peijs, T. (2004). Processing of all-polypropylene composites for ultimate recyclability. *Proceedings of the Institution of Mechanical Engineers Part L–Journal of Materials-Design and Applications, 218*(L2), 145–155.

Chermant, J. L., Fantozzi, G., & Naslain, R. (2000). Composite materials for aeronautical and aerospace applications – Introduction. *Annales De Chimie – Science Des Materiaux, 25*(7), 515–516.

Cuculo, J. A., Smith, C. B., Sangwatanaroj, U., Stejskal, E. O., & Sankar, S. S. (1994). A study on the mechanism of dissolution of the cellulose/NH_3/NH_4SCN system. 1. *Journal of Polymer Science Part A Polymer Chemistry, 32*(2), 229–239.

Egusa, S., Kitaoka, T., Goto, M., & Wariishi, H. (2007). Synthesis of cellulose in vitro by using a cellulase/surfactant complex in a nonaqueous medium. *Angewandte Chemie International Edition, 46*(12), 2063–2065.

Gindl, W., & Keckes, J. (2005). All-cellulose nanocomposite. *Polymer, 46*(23), 10221–10225.

Gindl, W., Martinschitz, K. J., Boesecke, P., & Keckes, J. (2006). Structural changes during tensile testing of an all-cellulose composite by in situ synchrotron X-ray diffraction. *Composites Science and Technology, 66*(15), 2639–2647.

Hattori, M., Koga, T., Shimaya, Y., & Saito, M. (1998). Aqueous calcium thiocyanate solution as a cellulose solvent. Structure and interactions with cellulose. *Polymer Journal, 30*(1), 43–48.

Heinze, T., Dicke, R., Koschella, A., Kull, A. H., Klohr, E. A., & Koch, W. (2000). Effective preparation of cellulose derivatives in a new simple cellulose solvent. *Macromolecular Chemistry and Physics, 201*(6), 627–631.

Hult, E. L., Iversen, T., & Sugiyama, J. (2003). Characterization of the supermolecular structure of cellulose in wood pulp fibres. *Cellulose, 10*(2), 103–110.

Klemm, D., Heublein, B., Fink, H. P., & Bohn, A. (2005). Cellulose: Fascinating biopolymer and sustainable raw material. *Angewandte Chemie International Edition, 44*(22), 3358–3393.

Klemm, D., Schumann, D., Kramer, F., Hessler, N., Hornung, M., Schmauder, H. P., et al. (2006). Nanocelluloses as innovative polymers in research and application. In *Polysaccharides II* (pp. 49–96). Berlin: Springer-Verlag.

Lu, X., Zhang, M. Q., Rong, M. Z., Shi, G., & Yang, G. C. (2002). All-plant fiber composites. I: Unidirectional sisal fiber reinforced benzylated wood. *Polymer Composites, 23*(4), 624–633.

Lu, X., Zhang, M. Q., Rong, M. Z., Yue, D. L., & Yang, G. C. (2004). Environmental degradability of self-reinforced composites made from sisal. *Composites Science and Technology, 64*(9), 1301–1310.

McCormick, C. L., Callais, P. A., & Hutchinson, B. H. (1985). Solution studies of cellulose in lithium-chloride and *N,N*-dimethylacetamide. *Macromolecules, 18*, 2394.

Miravete, A. (1997). Composite materials in building: Introduction. *Materiales De Construccion, 47*(247–248), 5–9.

Moharram, M. A., & Mahmoud, O. M. (2007). X-ray diffraction methods in the study of the effect of microwave heating on the transformation of cellulose I into cellulose II during mercerization. *Journal of Applied Polymer Science, 105*(5), 2978–2983.

Nishino, T., & Arimoto, N. (2007). All-cellulose composite prepared by selective dissolving of fiber surface. *Biomacromolecules, 8*(9), 2712–2716.

Nishino, T., Matsuda, I., & Hirao, K. (2004). All-cellulose composite. *Macromolecules, 37*(20), 7683–7687.

Nishio, Y. (2006). Material functionalization of cellulose and related polysaccharides via diverse microcompositions. In *Polysaccharides II* (pp. 97–151). Berlin: Springer-Verlag.

Nishiyama, Y., Langan, P., & Chanzy, H. (2002). Crystal structure and hydrogen-bonding system in cellulose 1 beta from synchrotron X-ray and neutron fiber diffraction. *Journal of the American Chemical Society, 124*(31), 9074–9082.

Qin, C., Soykeabkaew, N., Xiuyuan, N., & Peijs, T. (2008). The effect of fibre volume fraction and mercerization on the properties of all-cellulose composites. *Carbohydrate Polymers, 71*(3), 458–467.

Soykeabkaew, N., Arimoto, N., Nishino, T., & Peijs, T. (2008). All-cellulose composites by surface selective dissolution of aligned ligno-cellulosic fibres. *Composites Science and Technology, 68*(10–11), 2201–2207.

Soykeabkaew, N., Nishino, T., & Peijs, T. (2009). All-cellulose composites of regenerated cellulose fibres by surface selective dissolution. *Composites Part A Applied Science and Manufacturing, 40*(4), 321–328.

Swatloski, R. P., Spear, S. K., Holbrey, J. D., & Rogers, R. D. (2002). Dissolution of cellulose with ionic liquids. *Journal of the American Chemical Society, 124*, 4974–4975.

Tsai, S. W., & Hahn, H. T. (1980). *Introduction to composite materials* (455 pp). Lancaster, PA: Technomic Publishing.

Yan, L. F., & Gao, Z. J. (2008). Dissolving of cellulose in PEG/NaOH aqueous solution. *Cellulose, 15*(6), 789–796.

Zhang, L. N., Ruan, D., & Zhou, J. P. (2001). Structure and properties of regenerated cellulose films prepared from cotton linters in NaOH/Urea aqueous solution. *Industrial & Engineering Chemistry Research, 40*(25), 5923–5928.

Zhao, Q., Yam, R., Zhang, B. Q., Yang, Y. K., Cheng, X. J., & Li, R. (2009). Novel all-cellulose ecocomposites prepared in ionic liquids. *Cellulose, 16*(2), 217–226.